Computation of electrical conductance in nano-scale junctions for device applications

2004 J. Phys.: Condens. Matter 16 S5563

(http://iopscience.iop.org/0953-8984/16/48/012)

INSTITUTE OF PHYSICS PUBLISHING JOURNAL OF PHYSICS: CONDENSED MATTER

J. Phys.: Condens. Matter **16** (2004) S5563–S5570 PII: S0953-8984(04)81257-8

Computation of electrical conductance in nano-scale junctions for device applications

J Inoue[1], H Itoh[1], S Honda[1], K Yamamoto[1] and T Ohsawa[2]

[1] Department of Applied Physics, Nagoya University, Nagoya 464-8603, Japan
[2] Venture Business Laboratory, Nagoya University, Nagoya 464-8603, Japan

Received 26 May 2004
Published 19 November 2004
Online at stacks.iop.org/JPhysCM/16/S5563
doi:10.1088/0953-8984/16/48/012

Abstract

Numerical results of electrical conductance and magnetoresistance of ferromagnetic tunnel junctions and semiconductor/semimetal junctions are presented, putting an emphasis on effects of disorder on the conductance. It is shown that the disorder strongly affects the tunnelling conductance and magnetoresistance. It is discussed how the interfacial resonant states appearing in semiconductor/semimetal junctions influence the conductance. Numerical simulation of diffusive conductivity of a two-dimensional electron gas with spin–orbit interaction is also performed, and the results are compared with the analytical result.

(Some figures in this article are in colour only in the electronic version)

1. Introduction

Nano-scale magnetoelectronics is a developing field of science and technology. Magnetoresistive phenomena, the giant magnetoresistance (GMR) [1] and tunnel magnetoresistance (TMR) [2, 3] have already been applied to magnetic sensors and random access memories. Semiconductor spintronics [4] also attracts much interest since the discovery of the high Curie temperature magnetic semiconductors (GaMn)As [5]. It is expected that the characteristic features of magnetic, transport, and optical properties of the new materials may generate novel functions in artificial nano-scale junctions. To this end, high quality junctions of nano-scale size have to be fabricated. Even for high quality samples, however, some effects of roughness might be unavoidable. In order to understand and/or predict the results of experiments, computational simulation using microscopic models may be a powerful tool. In other words, this kind of computational simulation may be called device design, the importance of which may increase in the near future in addition to the material design.

In the calculation of the transport properties of junctions, one has to take several ingredients into consideration: complex structures of the junctions, electronic structures of different constituent materials, structural roughness or disorder near the interface. Quantum effects

become important for nano-scale junctions as well. In this paper, we present numerical results of electrical conductance (or conductivity) and magnetoresistance (MR) for junctions and two-dimensional (2D) systems, putting an emphasis on the effect of disorder on the conductance and MR. Because there is no translational invariance in junctions and in systems with disorder, we calculate the conductivity or conductance in a real space method, that is, using the recursive Green function method for the Kubo–Landauer formula [6, 7]. The disorder may be treated directly for finite size systems, or by using the coherent potential approximation. We will show that the effect of disorder is quite large especially for tunnel junctions.

In the next section, we deal with TMR oscillation in magnetic tunnel junctions, in which a spacer ferromagnetic layer is inserted by the tunnel barrier. In order to study the role of the interfacial electronic states on the conductance, we adopt semiconductor/semimetal junctions. In the third section, we study the diffusive transport in a 2D electron gas (2DEG) with spin–orbit interaction, and in double-layer manganites which include strong disorder.

2. Tunnel conductance in hetero-junctions

2.1. Ferromagnetic tunnel junctions

TMR oscillation has recently been observed for NiFe/Al–O/Cu/Co tunnel junctions as a function of the Cu layer thickness [8]. The TMR oscillates around zero with a period determined by the Fermi wavevector of Cu. Although a ballistic model for TMR [9] shows the oscillation of TMR, the theory predicts oscillation around a non-zero value of TMR ratio and complex periods of oscillation caused by both Cu Fermi wavevector and cut-off wavevector corresponding to the depth of the quantum well state formed for the minority spin states at the Cu layer. Thus the theory fails to explain the important characteristics of oscillation around zero TMR ratio and the period of the oscillation.

On the other hand, Itoh *et al* [10] have successfully explained the experimental observation by introducing the effects of disorder on the tunnel conductance. Although they have used a simple tight binding model, the results are applicable to real systems. The essence of the explanation is as follows. Because of the violation of the conservation law of the momentum $k_{\parallel}$ parallel to junction planes, tunnelling of electrons via quantum well states is allowed, which *increases* the tunnel conductance. The increase of tunnel conductance is larger in the anti-parallel (AP) alignment of the magnetizations of NiFe and Co layers than in parallel (P) alignment. That is, the effect of disorder is more effective in AP alignment than in P alignment because the Fermi surfaces of the left- and right-hand leads are different from each other in AP alignment. Momentum-resolved conductance calculated for clean and disordered junctions in AP alignment is shown in figure 1. Sharp peaks appearing in the conductance originate from disorder-induced tunnelling via quantum well states. Furthermore, the tunnelling via quantum well states makes the cut-off wavevector vague, and as a result it weakens the intensity of the oscillation caused by the cut-off wavevector. Thus, the TMR ratio oscillates around the zero value with a period determined solely by the Fermi wavevector of the Cu Fermi surface.

The present theory does not necessarily state that the TMR ratio always oscillates around the zero value. Let us consider Fe/Al–O/Fe/Cr type junctions. In this type of junction, the quantum well states appear at the Fe layer for the majority spin state (see the inset of figure 2). The mismatch of the electronic states of the left-hand ferromagnet (FM) and right-hand nonmagnet (NM) is larger in the majority spin state than in the minority spin state. Therefore, the disorder affects the tunnel conductance more strongly in the majority spin state than in the minority one, and increases the conductance in P alignment. The calculated results of the TMR ratio as a function of FM layer thickness are shown in figure 2. Here, the TMR

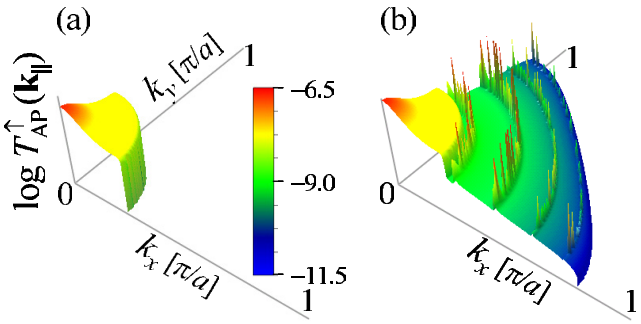

Figure 1. Momentum-resolved conductance in antiparallel alignment of the magnetizations. The conductance of the ↑-spin state is plotted as a function of the incident wavevector $\boldsymbol{k}_{\parallel}$ for (a) clean and (b) disordered junctions.

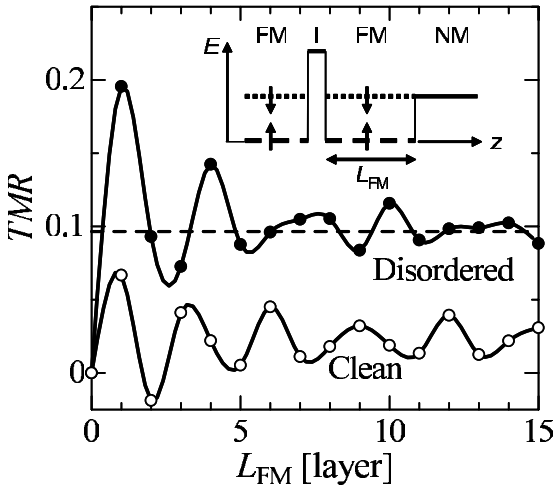

Figure 2. TMR ratio as a function of the ferromagnetic spacer layer thickness calculated for clean (open circles) and disordered (solid circles) FM/I/FM/NM junctions. The dashed horizontal line denotes the TMR ratio obtained for the FM/I/FM junction. Inset: schematic figure of potential profile in parallel alignment of magnetizations. The on-site potentials of FM for ↑- and ↓-spin states are indicated by dashed and dotted lines, respectively.

ratio is defined as

$$\mathrm{TMR} = \frac{\Gamma_{\mathrm{P}} - \Gamma_{\mathrm{AP}}}{\Gamma_{\mathrm{P}}}, \tag{1}$$

where Γ_{P} and Γ_{AP} are the tunnel conductance in P and AP alignments, respectively. The TMR ratio oscillates around a finite value because the barrier is sandwiched by two FMs in this case. The oscillation period is not single valued as can be seen in the figure. It is determined by both majority and minority Fermi wavevectors of FM.

The extrapolated value of TMR ratio onto thicker FM layers is shown by a broken line in figure 2. The value is nothing but the TMR ratio of FM/Al–O/FM junctions. This means that the disorder conceals the presence of the NM lead. In the junctions with a Cu inserted layer, the extrapolated value of TMR ratio is zero because the junction is of FM/Al–O/NM type. Thus, we may conclude that the TMR oscillates around a value determined by the barrier structure sandwiched by two materials, which may be a quite reasonable result.

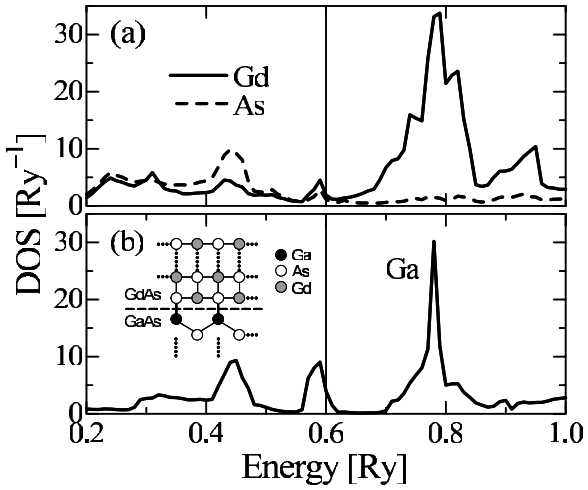

Figure 3. Local density of states of (a) Gd and As and (b) Ga at interface layers of GdAs/GaAs. GdAs of four atomic layers is stacked on semi-infinite GaAs(001). Thin vertical lines indicate the position of the Fermi energy. Inset: schematic diagram of GdAs/GaAs interface.

The result predicts an enhancement of TMR ratio for a suitable combination of ferromagnetic materials of tunnel junctions. Actually, the TMR ratio shown in figure 2 is enhanced at thin spacer FM layers. Recently, Nagahama *et al* [11] have observed an increase in the TMR ratio as a function of spacer Fe layer in Fe/Al–O/Fe/Cr tunnel junctions. No clear oscillation, however, has yet been observed in these tunnel junctions. Since the present study uses a simple model, no quantitative comparison between theoretical and experimental results is available at present.

2.2. Semiconductor/semimetal junctions

It is well known that interfacial states appear at the semiconductor interfaces. The interfacial states result from an interference of wavefunctions of s and p orbitals reflected by the interface or surface, and often called Shockley resonant states. In this paper, we show how these resonant states appear in GaAs/GdAs junctions, where GdAs is a semimetal, and study their effects on electrical transport by adopting a realistic tight binding model.

The parameter values of the sp^3 tight binding Hamiltonian for GaAs have been taken from Harrison's textbook [12] and those of the spd Hamiltonian for GdAs, which has NaCl type lattice structure, have been fitted to results obtained in the first principles band calculation [13, 14]. The electronic density of states (DOS) at the interface has been calculated for the GaAs/GdAs interface with Ga termination (see the inset of figure 3(b)).The calculated results of the DOS of Gd and As in the first interface layer of GdAs, and Ga in the first interface layer of GaAs, are shown in figures 3(a) and (b), respectively. The energy bandgap of GaAs opens around $E = 0.55$–0.65 Ryd. There is no energy gap in the DOS of GdAs because it is a semimetal. In the figure, we clearly see that the resonant state appears at the energy $E \sim 0.6$ Ryd, and extends slightly into the GdAs sites.

In order to study the effect of the resonant states on the electrical transport, we calculate the conductance for GaAs/GdAs/GaAs trilayers. The current flows perpendicular to the layer planes. The calculated results of the energy dependence of the conductance are shown in figures 4 for both Ga and As terminations. We see there is no peak in the conductance at the

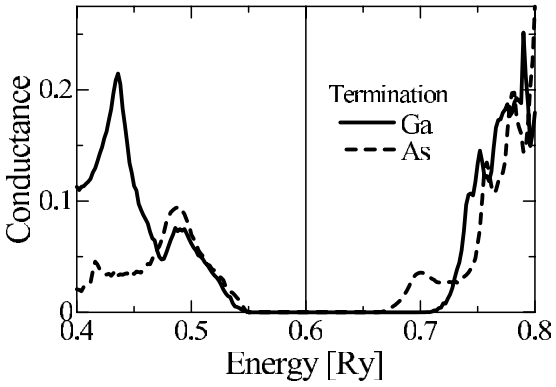

Figure 4. Conductance of GaAs/GdAs/GaAs trilayer. GdAs thickness is four atomic layers. Results obtained for Ga and As terminated junctions are plotted by solid and broken curves, respectively.

energy where the resonant states appear. The results are quite reasonable because the resonant states are localized at the interface, and do not extend through the whole region of GaAs, that is, the left and right leads attached. Therefore, they do not contribute to the conductance.

The interfacial states, however, may contribute to conductance when they mix with the extended states of the system. To illustrate this, we present results using the simplest model to produce the resonant state, 1D model using sp orbitals and metal/semiconductor/metal junctions [15]. In this case, the resonant state appears in the semiconductor layer and mixes with the extended states in metals. Furthermore, the resonant states on both interfaces interfere and split into two peaks. Numerical results of DOS are shown in figure 5(a). Corresponding results of the conductance are shown in figure 5(b). The results may indicate that the resonant states give rise to a strong influence on the conductance when the Fermi energy is located near the resonant states, and when the resonant states mix with the extended states due, for example, to roughness.

3. Conductivity in two-dimensional systems

3.1. 2DEG

A two-dimensional electron gas (2DEG) with spin–orbit (SO) interaction attracts much interest [16, 17] because the electric transport in a 2DEG is influenced by the intrinsic spin degree of freedom caused by the SO interaction [18]. Recently, longitudinal conductivity σ in the diffusive regime has been studied for isotropic short-range scatterers [19, 20]. It has been shown that σ increases in a quadratic way with increasing SO interaction λ,

$$\sigma = \sigma_{\mathrm{D}} + e^2 D\tau\lambda^2, \tag{2}$$

where σ_{D} is the Drude conductivity and e, D, and τ are the electric charge, density of states at the Fermi level of the 2DEG, and lifetime, respectively. The expression has been derived in the Born approximation with an assumption that the lifetime broadening of the energy levels is smaller than the SO splitting of the band. In this paper we perform numerical simulation of the longitudinal conductivity in the diffusive regime by adopting isotropic and short-range scatterers, and compare the result with equation (2). The work may be useful to study the reliability of the analytical results and the finite size effects on the conductivity.

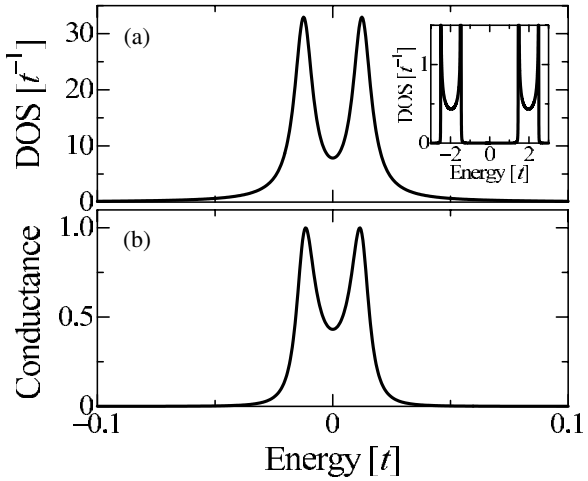

Figure 5. Local density of states (a) and conductance (b) calculated for a 1D metal/semiconductor/metal junction. In (a), the density of states at the first interface layer of the semiconductor is shown. Inset of (a): density of states of the bulk semiconductor.

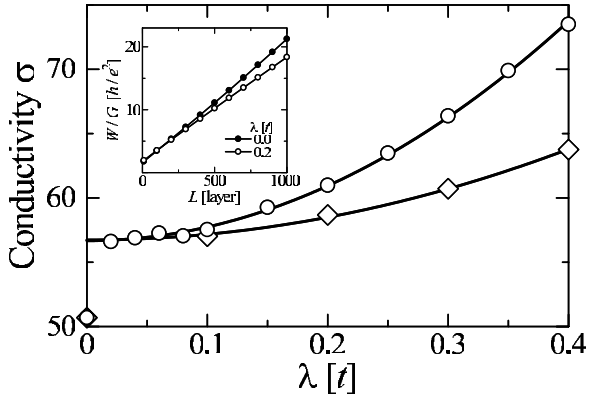

Figure 6. Conductivity as a function of the spin–orbit interaction λ. Open circles and diamonds are obtained for fixed Fermi energy and for fixed electron number, respectively. Inset: inverse of conductance as a function of the sample length.

To make the numerical simulation for finite size lattices feasible, we transform the 2DEG Hamiltonian into a lattice model characterized by electron hopping t between nearest neighbour sites and SO interaction λ [21]. In order to deduce the electrical conductivity σ in the diffusive regime from the conductance Γ calculated for finite size lattices, we use the following relation:

$$\frac{1}{\Gamma} = R_{\mathrm{C}} + \frac{1}{\sigma}\frac{L}{W}, \tag{3}$$

where R_{C} is a contact resistance and L and W are sample length and width, respectively. The second term represents Ohmic resistivity being proportional to L. Therefore, we get the value of σ from the slope in the $1/\Gamma$ versus L plot as shown in the inset of figure 5. In practice, we evaluate the value of σ from the slope between $L = 200$ and 1000. The value of $W = 200$ is used throughout the calculations. The Fermi wavelength and mean free path are about 6 and 48, respectively, in units of the lattice constant for parameter values used in the simulation.

The calculated results are shown in figure 6, where open circles are results for a fixed value of Fermi energy E_F and diamonds are those for a fixed number of electrons. The results indicate clearly the quadratic dependence of σ on the SO interaction λ, $\sigma = c_1 + c_2\lambda^2$, in agreement with the analytical results, equation (2). To see this more clearly, we compare the ratio $\gamma \equiv c_1/c_2$ with the analytical one. The results of σ for a fixed E_F give $\gamma \sim 0.55 \pm 0.1$ and those for a fixed number of electrons give about one-half of this value. The analytical result gives $\gamma = 1/2$. This value corresponds to that for fixed E_F because σ_D and $e^2 D\tau$ in equation (2) are determined for 2DEG without SO interaction. Therefore the agreement between analytical and simulated results is quite sufficient. The coefficients σ_D and $e^2 D\tau$, however, are dependent on SO interaction since the electronic states and E_F varied with SO interaction. Once we take this effect properly, a smaller value of γ should be obtained in the analytical expression.

3.2. Double-layer manganites

Numerical simulation of conductivity as shown in the previous subsection may be applied to double-layer manganites, in which double MnO layers are separated from other layers. A realistic but simple model for manganites is a tight binding model of e_g orbitals with Hund coupling between e_g electron spins and localized t_{2g} spins with $S = 3/2$ [22]. One may replace the spin fluctuation of the localized spins with static random potentials with suitable probabilities. When we adopt this model of *alloy analogy*, the numerical simulation of the conductivity becomes possible. In this case, however, one should be careful of the localization effect as the random potentials are rather strong. Numerical simulation of this kind is now in progress.

4. Summary

We have presented numerical results of electrical conductance and magnetoresistance of ferromagnetic tunnel junctions, semiconductor/semimetal junctions, and a two-dimensional electron gas putting an emphasis on effects of disorder on the conductance. It is shown that the tunnelling conductance may be strongly affected by the presence of disorder, and that the disorder is crucial to explain the TMR oscillation observed recently for eptaxial samples. It is shown that interfacial resonant states appearing in semiconductor/semimetal junctions may contribute to conductance when they mix with the extended states. Numerical simulation of diffusive conductivity of a two-dimensional electron gas with spin–orbit interaction is performed. The calculated results are in good agreement with the analytical result. A possible application of the numerical simulation to double-layer manganites has been briefly described.

Acknowledgments

JI is grateful for financial support provided by the NEDO International Joint Research Project (NAME), FEMD-CREST, a Grant-in-Aid for Scientific Research in Priority Areas 'Semiconductor nanospintronics' of The Ministry of Education, Culture, Sports, Science, and Technology, Japan, and NAREGI.

References

[1] Baibich M N, Broto J M, Fert A, Van Dau F N, Petroff F, Etienna P, Creuzet G, Freiderich A and Chazelas J 1988 *Phys. Rev. Lett.* **61** 2472
[2] Miyazaki T and Tezuka N 1995 *J. Magn. Magn. Mater.* **139** L231

[3] Moodera J S, Kinder L R, Wong T M and Meservey R 1995 *Phys. Rev. Lett.* **74** 3273
[4] Wolf S A, Awschalom D D, Buhrman R A, Daughton J M, von Molnar S, Roukes M L, Chtchelkanova A Y and Treger D M 2001 *Science* **294** 1488
[5] Ohno H, Shen A, Matsukura F, Oiwa A, Endo A, Katsumoto S and Iye Y 1996 *Appl. Phys. Lett.* **69** 363
Ohno H 1998 *Science* **281** 951
[6] Itoh H, Kumazaki T, Inoue J and Maekawa S 1998 *Japan. J. Appl. Phys.* **37** 5554
[7] Itoh H, Shibata A, Kumazaki T, Inoue J and Maekawa S 1999 *J. Phys. Soc. Japan* **69** 1632
[8] Yuasa S, Nagahama T and Suzuki Y 2002 *Science* **297** 234
[9] Mathon J and Umerski A 1999 *Phys. Rev.* B **60** 1117
[10] Itoh H, Inoue J, Umerski A and Mathon J 2003 *Phys. Rev.* B **68** 174421
[11] Nagahama T, Yuasa S, Suzuki Y and Tamura E 2001 *Appl. Phys. Lett.* **79** 4381
[12] Harrison W A 1980 *Electronic Structure and the Properties of Solids* (New York: Freeman)
[13] Xia J-B, Ren S-F and Chang Y-C 1991 *Phys. Rev.* B **43** 1692
[14] Petukhov A G, Lambrecht W R L and Segall B 1996 *Phys. Rev.* B **53** 4324
[15] Foo E-Ni and Wong H-S 1974 *Phys. Rev.* B **9** 1857
[16] Murakami S, Nagaosa N and Zhang S-C 2003 *Science* **301** 1348
[17] Sinova J, Cultcer D, Niu Q, Sinitsyn N A, Jungwirth T and MacDonald A H 2004 *Phys. Rev. Lett.* **92** 126603
[18] Rashba E I 1960 *Fiz. Tverd. Tela* **2** 1224
Rashba E I 1960 *Sov. Phys.—Solid State* **2** 1109 (Engl. Transl.)
Bychkov Yu A and Rashba E I 1984 *Pis. Zh. Eksp. Teor. Fiz.* **39** 66
Bychkov Yu A and Rashba E I 1984 *JETP Lett.* **39** 78 (Engl. Transl.)
[19] Inoue J, Bauer G E W and Molenkamp L W 2003 *Phys. Rev.* B **67** 033104
[20] Inoue J, Bauer G E W and Molenkamp L W 2004 *Phys. Rev.* B at press
[21] Pareek T P and Bruno P 2002 *Phys. Rev.* B **65** R241305
Pareek T P 2004 *Phys. Rev. Lett.* **92** 076601
[22] Inoue J and Maekawa S 1995 *Phys. Rev. Lett.* **74** 3407 and references therein